JOURNAL OF CATALYSIS 141, 612–627 (1993)

Transient Kinetic Study of the Reaction of CH_4 and C_2H_6 with the Lattice Oxygen of Li^+-Doped TiO_2 Catalyst

A. M. EFSTATHIOU, D. PAPAGEORGIOU, AND X. E. VERYKIOS

Institute of Chemical Engineering and High Temperature Chemical Processes, Department of Chemical Engineering, University of Patras, GR-26500, Patras, Greece

Received November 6, 1992; revised January 29, 1993

A transient kinetic study of the reaction of CH_4/He and C_2H_6/He with the lattice oxygen of Li^+-doped TiO_2 catalyst was performed. The results obtained indicate that lattice oxygen species must be considered as oxidation sites for both CH_4 and C_2H_6 molecules leading mainly to the formation of gas-phase CO_2. It was also found that more than one kind of carbon species accumulate on the catalyst surface in large quantities, following reaction with C_2H_6/He mixture in the range 700–845°C, a result opposite to that found with the CH_4/He mixture. The amount of these carbon species removed by reaction with gas-phase oxygen (O_2 titration) was found to strongly depend on the temperature of titration. A kinetic model, based on a sequence of elementary steps is proposed to interpret the transient oxygen titration results. An activation energy of 15.3 kcal · mol^{-1} for the reaction of carbon species with gas-phase oxygen is estimated. Activation energies of 34 and 28 kcal · mol^{-1} for CH_4 and C_2H_6 reactions with lattice oxygen, respectively, are calculated from initial rates.

INTRODUCTION

The oxidative coupling of methane to ethane and ethylene has become a subject of intense research worldwide. A large number of oxide systems has been tested so far, and review papers which summarize the results obtained have appeared in the literature (*1–5*). Most of the literature reports on this subject are devoted to the activity and C_2-selectivity properties of different catalysts with the goal to achieve C_2-yields of practical interest. Less attention has been given to the elucidation of the elementary steps of methane dimerization and formation of undesired CO_x ($x = 1, 2$) products over many catalysts studied. In particular, there is no conclusive evidence concerning the actual role of lattice oxygen species as compared to that of other adsorbed oxygen species formed during reaction conditions (*5, 6*).

The steady-state tracing technique (*7, 8*) which allows the *in situ* measurement of surface intermediate species and their reactivities, has recently been applied on some catalytic systems for the oxidative coupling of methane (*9–14*). For all the catalyst formulations studied, it was found that the coverage of adsorbed methane under reaction conditions is practically zero. However, there is a large reservoir of oxygen species (several monolayers) which participate in the formation of CO and CO_2. The coverage of the precursor intermediate species that leads to C_2H_6 is also small (*11, 14*).

Some basic reaction steps may be similar over many catalyst systems studied, but a controversy on other mechanistic steps exists. The basic initial reaction step is generally agreed to be the hydrogen abstraction from the methane molecule by the aid of surface oxygen anion species (*15–17*). The production of methyl species in such a process, and the subsequent release of these into the gas phase to form ethane, has been probed (*15, 18*). On the other hand, evidence has been provided for the formation of C_2H_6 on the catalyst surface in addition to that in the gas phase (*11*). Other mechanistic steps

0021-9517/93 $5.00

on which a controversy exists are those leading to CO and CO_2. Under oxidative coupling of methane conditions, it is not yet clear whether CO and CO_2 arise from the oxidation of C_2H_6 and C_2H_4 in the gas phase, or surface elementary reactions leading to CO_x are also important. For the latter, it is still not clear whether lattice oxygen species or adsorbed oxygen species (formed under CH_4/O_2 conditions) or both contribute to the formation of CO and CO_2.

It has been demonstrated in our laboratory (*19–21*) that Li^+-doped TiO_2 is an effective catalyst for oxidative coupling of methane, giving rise to appreciable yield of C_{2+}-hydrocarbons. Lane *et al.* (*22*) have also studied the Li/TiO_2 system under oxidative coupling of methane conditions. However, their catalyst is rather considered as a Li^+-promoted TiO_2 as it has been discussed in a work recently reported (*19*).

In the present work the kinetics of interaction of CH_4 and C_2H_6 with the lattice oxygen of a Li^+-doped TiO_2 catalyst is studied using transient methods with on-line mass spectrometry. The objectives are (a) to examine the reactivity of lattice oxygen species alone (in the absence of gas-phase oxygen) towards the reactant CH_4 and the major product molecule C_2H_6, of the CH_4/O_2 reaction, and (b) to characterize the carbonaceous species left on the catalyst surface after CH_4/He and C_2H_6/He reaction by O_2 titration transient experiments. It is hoped that the present results will contribute towards a better understanding of the individual role that lattice oxygen and various other adsorbed oxygen species (formed under CH_4/O_2 conditions) play on the reaction of the oxidative coupling of CH_4 with Li^+-doped TiO_2 catalyst. The role of adsorbed oxygen species formed under CH_4/O_2, C_2H_6/O_2, and C_2H_4/O_2 reaction conditions can be best studied by steady-state tracing techniques (*11, 13, 14, 23*). Experimental work on this issue has recently been performed (*24, 25*). The present results are discussed in relation to catalytic results obtained on the same system (*19–21*).

EXPERIMENTAL

(*a*) *Preparation and Characterization of Li^+-Doped TiO_2 Catalyst*

Lithium-doped TiO_2 catalyst was prepared by the method of high temperature diffusion. Lithium nitrate was used as precursor of the doping Li^+ cation in an appropriate amount so as to yield 2 wt% lithium concentration (based on $Li_2O/(Li_2O + TiO_2)$). The precursor was mixed with TiO_2 (Degussa P-25) in a beaker containing distilled water. The slurry was heated under continuous stirring to evaporate the water, and the residue was further heated at 110°C overnight. The solid material obtained was crushed and sieved to about 48 mesh, placed in a ceramic tube and then fired in air at 900°C for 6 h. The firing procedure involved placing the ceramic tube in a furnace and heating at a rate of 15°C/min to 900°C, maintaining at this temperature for 6 h and then allowing it to slowly cool to room temperature.

The BET surface area of the catalyst was found to be ca. 0.2 m^2/g. Other characterization measurements performed on the present catalyst, such as electrical conductivity, surface acidity and basicity, XRD, and XPS, have been reported elsewhere (*19*).

(*b*) *Catalyst Treatment*

Before any measurements were obtained, the catalyst sample (1 g) was treated with pure oxygen at 800°C for 2 h. Between successive transient experiments with CH_4/He and C_2H_6/He mixtures, the catalyst sample was treated with a 10% O_2/He mixture at 800°C for 30 min in order to establish approximately a similar initial surface state. It was determined experimentally that oxygen treatments at 800°C for a time greater than 30 min did not influence the transient results.

(*c*) *Flow-System for Transient Studies*

An appropriate flow system that allows the application of transient methods (abrupt switches in the feed gas composition) was

employed in the present investigation. The main design features of this system are similar to those which have been described in detail elsewhere (*26–28*). Chemical analysis of the gases during transients is done by on-line mass spectrometer (VG Quadrupoles, Sensorlab 200 D) equipped with a fast response inlet capillary system. The desired gas mixtures are made up in a separate preparation apparatus and not by continuous blending of two streams to avoid mainly changes in gas composition by switching the valves (*26*). Calibration of the mass spectrometer is performed based on a prepared mixture of a known composition. The output signal from the mass spectrometer detector is then converted to mole fraction versus time by appropriate software. Methane, ethane, and carbon dioxide were recorded at the mass numbers of 15, 30, and 44, respectively. All gases were used at the flow rate of 30 ml/min (ambient).

The reactor used in this study consists of two 4.0-mm-i.d. sections of quartz tubes which serve as inlet and outlet to and from a quartz cell of 7.0 mm i.d. (nominal volume 2 ml). The entrance to the reactor cell was machined in such a way as to create a local gas mixing. The behavior of the entire reactor cell is close to that of a CSTR, as evidenced by the Ar response signal, following the switch He → Ar/He, and the analysis presented elsewhere (*27, 28*). Heating was provided by a small furnace controlled by a programmable temperature controller (Omega Engineering Inc., CN-2010). The temperature of the catalyst is measured by a K-type thermocouple placed within a quartz capillary well in the middle of the catalyst bed.

RESULTS

(*a*) *CH_4/He Reaction*

Figure 1 shows transient responses of gas-phase CO_2 at various temperatures between 760 and 845°C, following the switch: He → 5% CH_4/He (*t*), where *t* designates the real time of the experiment. As the CH_4/He mixture starts to flow over the catalyst, an initial

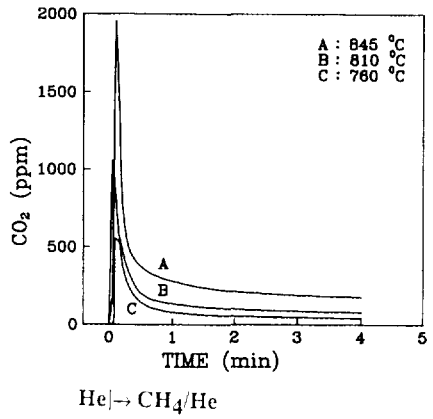

FIG. 1. Transient response of CO_2 under CH_4/He flow according to the delivery sequence: He → 5% CH_4/He (*T,t*). Curve A, T = 845°C; curve B, T = 810°C; and curve C, T = 760°C.

transient (spike) of the rate of production of CO_2 is obtained. This initial rate is found to increase with temperature. Following the initial transient response, the surface reaction dynamics lead to a rapid (within 30 s) decrease of the CO_2 production, following which the value of the latter decreases slowly during the remaining period of the experiment (a pseudosteady state is obtained). It is important to note that neither C_2H_6, C_2H_4, nor CO was found to be produced during the transients of Fig. 1. In addition to CO_2, H_2O was also detected and measured. Due to adsorption of H_2O in the source of the mass spectrometer, the quantitative analysis of the H_2O response and interpretation of its transient is difficult, if not impossible. Integration of the transients of Fig. 1 provides the amounts of CO_2 produced (up to the time where less than 50 ppm of CO_2 are measured), and these are given in Table 1. An equivalent amount of lattice oxygen species (monolayers) removed by the reaction as CO_2 during the experiments of Fig. 1 can also be calculated, and this is also given in Table 1. A monolayer of equivalent oxygen species is defined as the amount of oxygen species (μmol/g) present on the catalyst surface and is calculated based on the BET surface area (0.2 m^2/

TABLE 1

Amounts of CO_2 and Carbonaceous Species Produced during CH_4/He and C_2H_6/He Reaction with the Lattice Oxygen of Li^+-Doped TiO_2 Catalyst as a Function of Temperature

	CH_4/He		C_2H_6/He		
	CO_2		CO_2		Carbonaceous species accumulated
T (°C)	(μmol/g)	equivalent oxygen (monolayers)/g	(μmol/g)	equivalent oxygen (monolayers)/g	(μmol/g)
705	—	—	15.5	5.7	160
745	—	—	30.9	11.3	340
760	0.43	0.15	—	—	—
780	0.48	0.18	36.3	13.2	410
810	0.78	0.29	—	—	—
845	1.80	0.65	43.3	16.0	500

g), the lattice parameters, and the number of surface oxygen atoms/unit cell of rutile titania.

The initial rates (spikes) of CO_2 and those after 4 min of reaction (under pseudo steady state condition) shown in Fig. 1, were used to calculate activation energies for the reaction of CH_4 with the lattice oxygen. Figure 2, curve (a) shows the results of the logarithm of the initial rate vs $1/T$ in an Arrhenius plot from which a value of 34.6 kcal · mol^{-1} is obtained. A value of 36 kcal · mol^{-1} is obtained from pseudosteady state results,

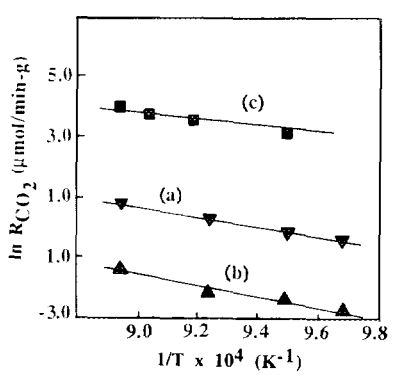

FIG. 2. Arrhenius plots of the rate of CO_2 production after CH_4/He (curves a and b) and C_2H_6/He (curve c) reaction with the lattice oxygen of Li^+-doped TiO_2 catalyst.

which are also shown in Fig. 2, curve (b). Initial rates of production of CO_2 from reaction of CH_4 with lattice oxygen are determined based on the appropriate material balance for a CSTR reactor. At the peak maximum shown in the transient results of Fig. 1 the accumulation term is zero, and therefore the outlet from the reactor molar rate of CO_2 is equal to the rate of production of CO_2 by reaction.

(b) C_2H_6/He Reaction

(b1) Effects of temperature. Figures 3a–3c show transient responses of gas-phase CO_2 at 705, 745, and 845°C, respectively, following the switch: He → 10% C_2H_6/He(t). At the lowest temperature studied, 705°C (Fig. 3a), there is an initial sharp increase (spike, peak 1) in the rate of production of CO_2 as the C_2H_6/He mixture starts to flow over the catalyst. This is followed by a quick achievement of a constant value of the rate of production of CO_2 which lasts for about 4 min. Then, the rate of reaction goes through a second overshoot (spike, peak 2), much larger than the first one, which decays to the former value (that obtained after 4 min of reaction) within about 2 min. Following this second peak in the rate of production of CO_2, a third small

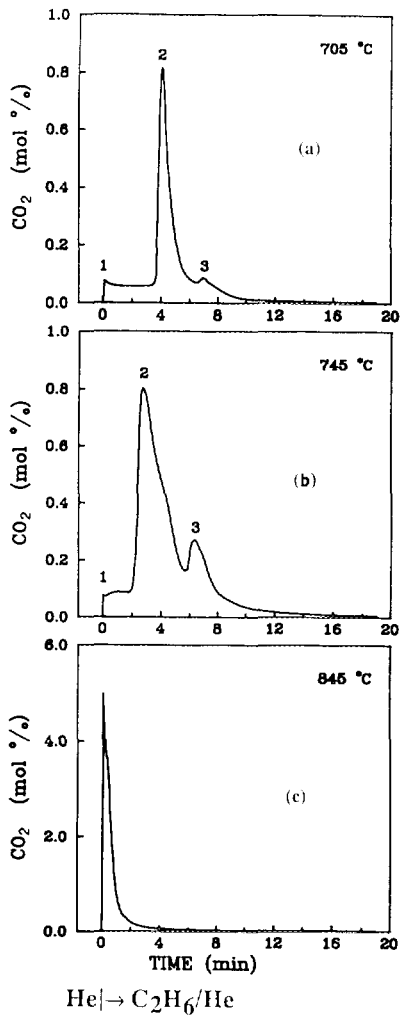

FIG. 3. Transient response of CO_2 under C_2H_6/He flow according to the delivery sequence: He → 10% C_2H_6/He (T,t); (a) T = 705°C, (b) T = 745°C, and (c) T = 845°C.

peak (peak 3) also appears after about 7 min of reaction, and the rate of CO_2 formation decays to essentially zero approximately 14 min after initiation of the experiment.

Increasing the temperature to 745°C (Fig. 3b), the second and third peaks observed at the lower temperature of 705°C grow in intensity, the peak maxima shift to shorter reaction times, and the intensity of first peak (spike) is also increased compared to that observed at 705°C. Further increase of the reaction temperature in the range 780–845°C results in the disappearance of the second and third peaks. At these temperatures only a single peak is obtained with a peak maximum at reaction time in the range t = 0–10 s. On the other hand, the quantity of CO_2 produced increases compared to that obtained at the lower temperatures. Figure 3c shows such a CO_2 transient response at 845°C. Integration of the transients of Fig. 3 gives the amount of CO_2 produced (μmol/g) and that of lattice oxygen consumed (monolayers). These are also shown in Table 1. It is noted that in the experiments of Fig. 3 small amounts of CH_4 and C_2H_4 were also measured (less than 10% of the CO_2 produced) in the range 780–845°C. As shown later, during the transient reaction of Fig. 3 carbon species accumulate on the catalyst surface. The amount of the latter can be calculated based on a carbon material balance. Thus, the amount of carbon species is found by subtracting from the amount of C_2H_6 consumed the amount of CO_2, CH_4, and C_2H_4 produced in the gas phase. The amount of C_2H_6 consumed is calculated from the area difference between the experimental C_2H_6 response and that of an inert Ar gas (*28*). The amount of carbonaceous species (μmol/g) accumulated on the catalyst at 705, 745, and 845°C are also given in Table 1.

The CO_2 transient results in the temperature range of 780–845°C, where only one peak is obtained, were used to calculate the apparent activation energy of the reaction of C_2H_6 with the lattice oxygen species of Li^+-doped TiO_2 catalyst to form CO_2. The observed logarithm of the initial rates of CO_2 production are shown as a function of the inverse temperature in an Arrhenius plot in Fig. 2, curve (c). From this plot, an activation energy of 28 kcal · mol^{-1} is calculated. This value is lower by 8 kcal/mol of the corresponding value obtained for the reaction of CH_4 with the catalyst surface.

The much greater extent of reaction of C_2H_6 than CH_4 with the lattice oxygen of

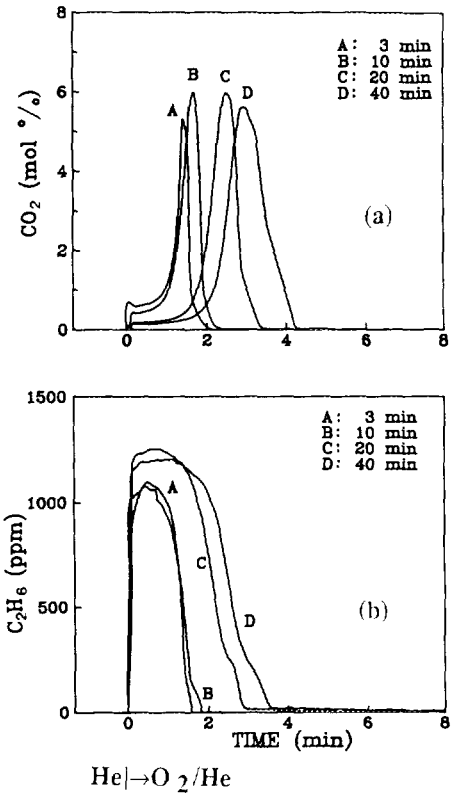

FIG. 4. (a) Transient response of CO_2 under O_2/He flow according to the delivery sequence: C_2H_6/He (845°C, Δt) → He (845°C, 180 s) → O_2/He (t). Curve A, Δt = 3 min; curve B, Δt = 10 min; curve C, Δt = 20 min, and curve D, Δt = 40 min. (b) Transient response of C_2H_6 obtained during O_2/He treatment according to the delivery sequence given in (a).

Li^+-doped TiO_2 catalyst was further investigated with respect to (a) effects of time on stream of C_2H_6/He and (b) oxygen titration of the carbon species produced by the C_2H_6/He reaction with the catalyst as well as their reactivity.

(b2) Effects of time on stream of C_2H_6/He at 845°C. Figures 4a and 4b show transient responses of gas-phase CO_2 and C_2H_6, respectively, at 845°C following the sequence: 10% C_2H_6/He (845°C, Δt) → He (845°C, 3 min) → 10% O_2/He (845°C, t). Results are given for times on stream of C_2H_6/He, Δt, between 3 and 40 min. The transient responses shown in Figs. 4a and 4b correspond to the 10% O_2/He treatment of the catalyst for the above-described gas delivery sequence. As time on stream increases, the amounts of CO_2 and C_2H_6 produced increase and a shift in the appearance of the maximum of the CO_2 peak (Fig. 4a) towards higher reaction times in oxygen flow is observed. The latter result is discussed later in relation to a kinetic model which is developed. Worth of noting is the broad peak of C_2H_6 (Fig. 4b) and the absence of a shift in the peak maximum of it, results opposite to those observed for CO_2 (Fig. 4a). The amounts of CO_2 and C_2H_6 produced (μmol/g) are shown in Table 2.

(b3) Effects of temperature during O_2/He treatment. The transient kinetics of the reaction of carboneceous species with oxygen, the former produced by reaction of C_2H_6/He with the lattice oxygen of the catalyst, was studied as follows: The catalyst was first treated with C_2H_6/He at 845°C for 10 min, followed by cooling of the reactor in He flow to a given temperature. The feed was then changed to O_2/He and the gas phase responses of the reaction products were monitored by mass spectrometry. Only CO_2 and small amounts of C_2H_6 were measured. These transients are presented in Figs. 5a and 5b for CO_2 and C_2H_6, respectively.

In Fig. 5a it is observed that upon switching to the O_2/He mixture a rapid increase in the rate of production of CO_2 is obtained, which decreases with increasing reaction temperature. In addition, the total amount

TABLE 2

Amounts of CO_2 and C_2H_6 Produced during O_2 Titration at 845°C, Following Reaction in C_2H_6/He at 845°C for Various Times on Stream

Time on stream (min)	CO_2 (μmol/g)	C_2H_6 (μmol/g)
3	46.8	1.6
10	48.0	1.7
20	64.0	3.3
40	79.5	4.0

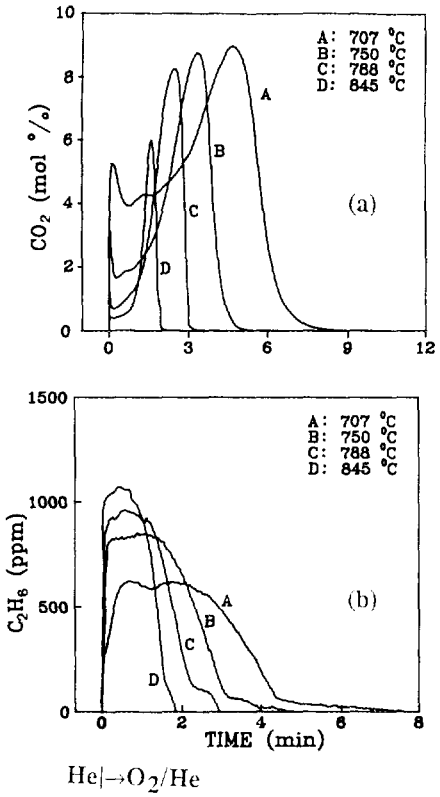

FIG. 5. (a) Transient response of CO_2 under O_2/He flow according to the delivery sequence: 10% C_2H_6/He (845°C, 600 s) → He, cool to reaction T → 10% O_2/He (T,t). Curve A, T = 707°C; curve B, T = 750°C, curve C, T = 788°C; and curve D, T = 845°C. (b) Transient response of C_2H_6 obtained during O_2/He treatment according to the delivery sequence given in (a).

of carbonaceous species removed by O_2, as CO_2, decreases significantly with increasing reaction temperature and a shift in the appearance of the CO_2 peak maximum towards shorter reaction times is observed. It is also noted that the shape of the CO_2 transient response is much affected by the temperature of reaction (Fig. 5a). The C_2H_6 response (Fig. 5b) is not the same as the CO_2 response. In this case the broadness of the peak maximum decreases with increasing reaction temperature, while peak maxima also shift towards shorter reaction times. The amounts of CO_2 and C_2H_6 produced (μmol/g) are shown in Table 3. The quantities of both species produced decrease significantly with increasing O_2 titration temperature.

TABLE 3

Amounts of CO_2 and C_2H_6 Produced during O_2 Titration at Various Temperatures, Following Reaction in C_2H_6/He at 845°C for 10 Min

O_2 titration temperature (°C)	CO_2 (μmol/g)	C_2H_6 (μmol/g)
707	455	2.7
750	238	2.5
788	145	2.1
845	48	1.6

(c) *Kinetic Model for the Oxidation of Carbonaceous Species Produced by C_2H_6/He Reaction*

To interpret the experimental results presented in Figs. 4 and 5, the following kinetic model is proposed. First, the surface carbonaceous species produced by the reaction of the C_2H_6 molecule with the lattice oxygen species are assumed to be of the CH_x (x = 0–3) and/or $-CH_xO$ (i.e., methoxy, x = 3) forms. The latter species (CH_xO) could also be formed during O_2 titration. The validity of this assignment is discussed later. Second, the formation of CO_2 occurs via a sequence of elementary steps, which are given below, where only those steps that control the overall reaction rate possess the same rate constant k. Third, the interaction of O_2 with the catalyst surface (creation of lattice and adsorbed oxygen), (step 1), is not considered as one of the rate-limiting steps, thus it is assumed to be at equilibrium. For the case of a CH_x species, steps 2–6 are appropriate:

$$O_2(g) + (2e^- \mid \square_s) \rightleftharpoons (O^{2-} \mid \square_s) + O(a) \quad \text{(step 1)}$$

$$CH_x(a) + O(s) \rightarrow CH_{x-1}(a) + OH(s) \quad \text{(step 2)}$$

$$CH_{x-1}(a) + O(s) \rightarrow CH_{x-2}(a) + OH(s) \quad \text{(step 3)}$$

$$CH_{x-2}(a) + O(s) \rightarrow CH_{x-3}(a) + OH(s) \quad \text{(step 4)}$$

$$C(a) + O(s) \rightarrow CO(a) + (s) \quad \text{(step 5)}$$

$$CO(a) + O(s) \rightarrow CO_2(g) + (s) \quad \text{(step 6)}$$

$$2\ OH(s) \rightarrow H_2O + O(s) + \square_s. \quad \text{(step 7)}$$

Here $\square_s$ is an oxygen vacancy, O^{2-} is a lattice oxygen species, O(a) is an adsorbed atomic oxygen species, $CH_x(a)$, $x = 1$–3 is an adsorbed hydrocarbon species, O(s) is an atomic oxygen site (lattice and/or adsorbed oxygen species), OH(s) is a hydroxyl species formed on an O(s) site, and (s) is a site. For the case of the presence of a CH_xO species, similar steps as those of 2–4 and 6 can be written, whereas step 5 may be absent from the above-described sequence of steps. Step 7 represents the formation of H_2O and the release of O(s) sites.

The rate of formation of CO_2 can be formulated according to *the number* of elementary steps among the steps 2–6 given above which control the overall reaction rate. With this in mind and the assumption that the surface concentration of O(s) species remains constant during oxygen titration, then analytical solutions for the rate of CO_2 formation exist. Recently, Bianchi and Gass (*29*) presented a similar analysis for the case of hydrogen titration of surface carbon species produced by the CO/H_2 reaction on an Fe/Al_2O_3 catalyst. The expressions for the characteristics of the maxima in the rate of CH_4 formation given by Bianchi and Gass (*29*) were found to be similar for the present CO_2 rate of formation according to the kinetic model described above. Of particular application to the present work is the relationship (*29*)

$$t_m = \frac{\alpha - 1}{k_0 \exp(-E/RT)[O_s]} \qquad (1)$$

where: t_m is the time of appearance of the peak maximum in the CO_2 response during O_2/He titration, α is the number of elementary steps with the same rate constant k, which control the rate of formation of CO_2, and $[O_s]$ is the concentration of O(s) species. The rate constant k is given by the Arrhenius relationship: $k = k_0 \exp(-E/RT)$, where E is the activation energy for the oxidation of $-CH_x$ or $-CH_xO$ species.

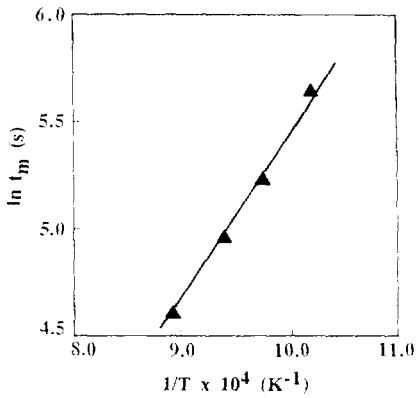

FIG. 6. Application of Eq. (2) for justifying the kinetic model derived for the oxidation of carbonaceous species formed by the reaction of C_2H_6 with the lattice oxygen of Li^+-doped TiO_2 catalyst.

Equation (1) shows that there exists a peak maximum at $t_m \neq 0$, if the rate of CO_2 formation is controlled by more than one steps ($\alpha > 1$). Equation (1) can be rearranged to give

$$\ln t_m = \ln\left(\frac{\alpha - 1}{k_0[O_s]}\right) + \left(\frac{E}{R}\right)\left(\frac{1}{T}\right). \qquad (2)$$

The validity of the kinetic model presented above was checked using Eq. (2) and the results of Fig. 5a. Figure 6 is a plot of these results based on Eq. (2). An activation energy of 15.3 kcal/mol for the oxidation of carbon species ($-CH_x$ or $-CH_xO$) to form CO_2 is estimated. The good fit of the data to the model is noted.

DISCUSSION

(a) CH_4/He Reaction

The transient kinetic results of the reaction of CH_4 and C_2H_6 molecules with the lattice oxygen of Li^+-doped TiO_2 catalyst to form CO_2 (Figs. 1–3) suggest the different characteristics of each reaction pathway (i.e., number of elementary steps, or rate-

determining step(s), or rate constants of individual reaction steps, or composition of surface intermediate species). The absence of gas-phase ethane product during reaction of CH_4 with the lattice oxygen of the catalyst (Fig. 1) is an important result. It has been suggested by many investigators, based on experimental evidence given by Lunsford and co-workers (*15, 18*), that in many catalysts used for oxidative coupling of methane (OCM), methyl radical species ($CH_3\cdot$), generated by the catalyst under OCM conditions (CH_4/O_2 feed) via H· abstraction from the CH_4 molecule by oxygen species, desorb into the gas phase to form C_2H_6. If this mechanistic step is correct, then the results of CH_4 reaction with the catalyst surface in the absence of gas-phase oxygen (Fig. 1) suggest that the rate of desorption of methyl radicals is much smaller than their rate of reaction to CO_2 on the catalyst surface, or $CH_3\cdot$ radicals desorb into the gas phase and form C_2H_6 which then burns on the catalyst surface. The second explanation is not plausible since no carbon deposits are left on the surface as in the case of C_2H_6 (Table 1). Furthermore, the transients of Figs. 1 and 3 are different. Thus, it is suggested that surface oxidation steps leading to CO_2 are dominant over the desorption of $CH_3\cdot$ species in the gas phase. These results then may imply that gas-phase oxygen is required in order to form adsorbed oxygen species on the surface which favor formation of $CH_3\cdot$ species with a desorption rate (leading to C_2H_6) comparable to that which leads to CO_x products. The present results of Fig. 1 suggest that following reaction of CH_4 (in the absence of gas-phase oxygen) with the catalyst surface, $-CH_x$ ($x = 0$–3) and/or $-CH_xO$ species are formed on the surface. These species react with the lattice oxygen of the catalyst to form exclusively CO_2. In particular, the formation of $-CH_3O$ (methoxy) species has been proposed as an intermediate species under OCM conditions on other catalytic systems (*30, 31*).

Ekstrom and Lapszewicz (*12*) have studied the reactivity of CH_4 with the lattice oxygen of Sm_2O_3, Li/Sm_2O_3, and Pr_6O_{11} catalysts using transient isotopic techniques. Their results indicated that the lattice oxygen of Sm_2O_3 was not reactive towards CH_4, whereas the opposite was true for Pr_6O_{11}. For the latter case, the CO_2 transients observed were very similar to those shown in Fig. 1.

The activation energy for the formation of CO_2 (34 kcal/mol), calculated from the CH_4 transient results of Fig. 1 as explained in a previous section, is similar in magnitude to that found under OCM conditions (38 kcal/mol) for the present catalyst (*19*). However, the activation energy of the reaction of C_2H_6 with lattice oxygen to form CO_2 was found to be smaller by 8 kcal/mol than that of the reaction of CH_4. On the other hand, recent transient work (*25*) with C_2H_6/O_2 mixtures provided the activation energy of reaction of C_2H_6 with adsorbed oxygen species (no gas-phase reaction) to be of 40 kcal/mol. These facts may imply that a large fraction of CO_2 produced under OCM conditions originates from the combustion of methyl radicals, which occurs via lattice oxygen species, and also from the combustion of C_2H_6 with adsorbed oxygen species. For the latter, experimental evidence using $^{13}C_2H_6$ has been provided recently by Nelson and Cant (*32*) over the Li/MgO catalyst. On the other hand, the combustion of C_2H_6 on lattice oxygen sites might be of secondary importance. Large amounts of carbon species accumulate on the catalyst during reaction with C_2H_6 in contrast to the case of CH_4. These results indicate that breaking of the C–H bond on the catalyst surface is more difficult than breaking of the C–C bond. However, the resulting carbon intermediate species from the reaction of CH_4 with the catalyst surface are more active towards lattice oxygen than the corresponding carbon species formed by the reaction of C_2H_6 with the surface.

The kinetic model developed to interpret the transient results of Fig. 5 assumes that the surface oxygen concentration remains constant during the oxidation steps 2–6.

Given the facts that: (a) only a small amount of carbon species is accumulated on the surface during reaction of CH_4 with the catalyst, (b) a small amount of equivalent oxygen is removed as CO_2 during the first 20 s of reaction (time required to form the peak maximum, spike in Fig. 1, followed by the rapid decay), and (c) diffusion of lattice oxygen species from the bulk to the surface does occur (*21*), it could be stated that during the initial 20 s of the transient the concentration of surface oxygen species remains approximately constant. Then, the appearance of the CH_4 peak maximum at $t = 0$ (spike in Fig. 1) at all temperatures studied suggests that the rate of oxidation of CH_x (x = 0–3) and/or $-CH_xO$ species according to the elementary steps 2–6 and Eq. (1) occurs via only *one rate-determining step*.

(b) C_2H_6/He Reaction

The isothermal transients of the reaction of C_2H_6 with the lattice oxygen species of the catalyst at 705°C (Fig. 3a) and 745°C (Fig. 3b) produced three peaks, whereas at 845°C only one peak is obtained. In attempting to understand these peaks and the sequence of steps for the oxidation of C_2H_6 by lattice oxygen species of the catalyst, a quantitative model should be used which must exactly describe these transients. However, such a task is not within the scope of this work. Only qualitative conclusions are drawn from the various peaks of Fig. 3.

Peak 1: The overshoot at time zero (peak 1) is in agreement with the initially high surface concentration of lattice oxygen species. In addition, this implies that the rate of oxidation of the various carbonaceous intermediate species that eventually lead to CO_2 is relatively fast.

Peak 2: The overshoot appearing as peak 2 in the temperature range of 705–780°C, which is much higher than that of peak 1, cannot possibly arise from an oxygen species of the same layer which is more reactive than that associated with peak 1. If this were the case, then one should expect that upon introducing C_2H_6 over the catalyst surface the more active oxygen species would react first. The following may be appropriate in trying to interpret the overshoot in peak 2.

The appearance of this overshoot coincides approximately with the depletion of the first equivalent monolayer of oxygen species of the catalyst. As oxygen atoms of the first layer are removed from the lattice of TiO_2, the corresponding lattice Ti^{4+} cations are reduced, and one expects that the strength of titanium and oxygen bond of the second layer would increase. During this destructive process of the surface of TiO_2, diffusion of lattice oxygen species from the bulk to the surface is expected, as it has been shown in a recent study by $^{18}O_2$ transient experiments (*21*). This diffusion process may result in an increase in the surface concentration of oxygen, if the rate of removal of surface oxygen by reaction is smaller than the rate of supply by diffusion. However, the surface concentration of oxygen would never exceed the value corresponding to the first atomic layer (before the catalyst is exposed to the C_2H_6/He reaction mixture). Therefore, the overshoot of peak 2, five times larger than that of peak 1, cannot be explained by a sudden increase in the surface concentation of oxygen.

Considering the rate of production of CO_2, R_{CO_2}, given by the relationship,

$$R_{CO_2} = k'\theta_C\theta_O, \qquad (3)$$

where k' is the rate constant, θ_C is the coverage of carbon-containing intermediate species formed by the reaction of C_2H_6 with the catalyst surface and which participate in the rate-determining step, and θ_O is the coverage of surface lattice oxygen species, and the considerations mentioned in the previous paragraph, then it is logical to think that the parameters θ_C and k' appeared in Eq. (3) must be responsible for the sudden increase in the rate of CO_2 formation (peak 2) observed.

It is appropriate to note here that catalytic rate enhancements during transient conditions have been observed in many systems. For example, oxidation of ethylene (*33*),

acetylene hydrogenation (*34*), ammonia synthesis (*35*) and carbon monoxide oxidation (*36–38*). A concept that has been proposed to explain this catalytic rate enhancements is that adsorbed intermediate species, which participate in the reaction, form islands (*39–42*). These islands are patches of the surface and reaction takes place along the perimeter of the island of the adsorbed reaction intermediate species. In the present work it was found that during the first 4 min of reaction (Fig. 3a), carbonaceous species build up on the surface. Their form by which are deposited on the surface is of course unknown. It is reasonable to suggest that in the present situation as well, during consumption of the first layer of surface lattice oxygen carbonaceous species accumulate in "island" forms on the catalyst surface. When a critical oxygen coverage occurs, by diffusion of lattice oxygen from the bulk, reaction occurs whose rate is enhanced dramatically due to high concentration of carbon species, and also to local increase of temperature from the exotherm of the combustion reaction. These processes give rise to peak 2 of Figs. 3a and 3b.

Similar overshoots in the rate of reaction have been observed for the CO/H_2 reaction on Rh/Al_2O_3 (*43*) and other catalysts. For the Rh/Al_2O_3 case it was found that the Rh surface appears deficient in hydrogen concentration following reaction in CO/H_2. Upon change of the feed from CO/H_2 to H_2, an overshoot in the rate of CH_4 production occurred, similar to that observed in the present work (Fig. 3, second peak). However, the CH_4 overshoot was explained, based on experimental evidence, as due to a sudden increase in the surface coverage of hydrogen.

Peak 3: The appearance of the third CO_2 peak (not a spike) in the transients of Figs. 3a and 3b, following that of the second peak described in the previous paragraphs, may have the same origin as that of the second peak. The magnitude of this peak is significantly smaller than that of the previous one due to the fact that the availability of mobile lattice oxygen is now limited since a large fraction of it has been consumed previously. This peak may also be attributed to oxidation of carbon species, formed in a previous reaction time, with a higher activation energy than that which gives rise to the second CO_2 peak.

The possibility that part of the CO_2 transient results in Figs. 3a and 3b could be explained as due to desorption of CO_2 as a result of readsorption effects along the catalyst bed, or from Li_2CO_3 decomposition, is excluded. This is based on the following experimental evidence. Transient experiments with 1.5% CO_2/He in the range 700–850°C showed that upon the switch from He to CO_2/He the gas phase response of CO_2 followed exactly that of an inert, nonadsorbing gas (Ar) when the switch from He to Ar/He in the range 700–850°C was made. This experiment clearly suggests that as far as the CO_2 is concerned there are no CO_2 readsorption effects in the results of Fig. 3. In addition, if any Li_2CO_3 is formed during the transient reaction of Fig. 3, the aforementioned transient results with CO_2/He suggest that the decomposition of Li_2CO_3 is a very fast process. Worth noting here are also results from transient isotopic experiments with $^{13}CH_4/^{18}O_2$ (*24*) which provided strong evidence that the carbon pool to form CO_2 during OCM reaction at 800°C is practically zero. This suggests that any appreciable amount of Li_2CO_3 reversibly interacting with gas phase CO_2 does not exist on the present Li^+-doped TiO_2 catalyst.

At temperatures in the range 780–845°C, reaction of C_2H_6 with lattice oxygen of the catalyst results in a single CO_2 peak only (Fig. 3c). This behaviour suggests that it is not possible, in this temperature range, to resolve the reaction processes which give rise to the second and third CO_2 peaks (Figs. 3a and 3b). The corresponding reaction rates become similar, and the plateau in the rate of CO_2 which appeared before the occurrence of the overshoot in peak 2 (Figs. 3a and 3b) disappears. The latter may be related to the dependence of island formation

of carbon species on reaction temperature. Thus, the single peak of Fig. 3c probably incorporates the three peaks of Figs. 3a and 3b. A noticeable break in the right-hand-side of the peak in Fig. 3c might indeed indicate this incorporation.

The amount of CO_2 produced during reaction of C_2H_6 with lattice oxygen is less than the total amount of equivalent oxygen present in the catalyst (0.35% of the total amount at 845°C). This, along with the fact that the reaction stops after a given time (see Figs. 3a–3c), may suggest that the carbonaceous species formed during reaction inhibit in some way the diffusion of bulk lattice oxygen to the surface or that the rate of diffusion of bulk lattice oxygen of lithium-doped titania which has been reduced to a considerable extent is immeasurably low. The possibility that destruction of the lattice may also play an inhibiting role for the aforementioned diffusion processes cannot be excluded. In addition, the release of O(s) by dehydroxylation of the surface to form H_2O (step 7) may be a slow enough reaction step compared to the other ones shown in the sequence of steps 2–6 of the model presented here, reducing, therefore, further reaction of C_2H_6 with lattice oxygen.

Morales and Lunsford (*44*) proposed the formation of $C_2H_5O^-$ species on the surface of MgO after reaction of the latter with C_2H_6. This ethoxide species may decompose to C_2H_4 or get oxidized to CO and CO_2. If such a species is formed on the present catalyst, then the predominant reaction route for this species is its oxidation to CO_2.

(*c*) *Oxidation of Carbonaceous Species Formed by C_2H_6/He Reaction with Lattice Oxygen of the Li^+-Doped TiO_2 Catalyst*

The kinetic model used for the oxidation of carbon species formed upon reaction of C_2H_6 with the lattice oxygen of Li^+-doped TiO_2 catalyst, based on a sequence of elementary steps, was found to explain well the shift, with respect to reaction time under oxygen flow, of the peak maximum obtained in the CO_2 transient response. The production of CO_2 during C_2H_6/He reaction (Fig. 3) certainly implies a breaking in the C–C bond of the ethane molecule, thus $-CH_x$ ($x = 0$–3) species are first expected to be formed. Further reaction of CH_x species with lattice oxygen to form a more stable CH_xO species is also possible. The present kinetic model, together with the experimental results of Fig. 5, for the first time provides information that accounts in some detail for the sequence of steps of the oxidation of carbon intermediate species formed by reaction of C_2H_6 with the lattice oxygen of an OCM catalyst.

It has been shown (*11*, *14*) and it has also been observed in this laboratory (*24*) that under OCM conditions the coverage of carbon-containing intermediate species that lead to CO and CO_2 is rather small. The transient responses (under steady-state tracing conditions) of $^{13}CO_2$ and ^{13}CO are relatively fast and close to the $^{13}CH_4$ response, so a detailed analysis of these transients by a model based on a sequence of elementary steps to probe for the mechanism of CO_x formation may not be feasible. On the other hand, the present transient results of Fig. 5 along with the kinetic model presented provide an alternative way to probe for the formation of CO_2 by the oxidation of carbonaceous species $-CH_x$ and/or $-CH_xO$, which are also likely to be formed under OCM conditions but with a very small coverage. Thus, the results of Figs. 5 and 6 may suggest that a stepwise dehydrogenation mechanism of an hydrogen-containing carbon intermediate species, formed under CH_4/O_2 reaction conditions by the aid of adsorbed oxygen species, to form CO and/or CO_2 may be operative. On the other hand, the results of Fig. 6 provide an activation energy of 15.3 kcal/mol for the formation of CO_2, based on the stepwise dehydrogenation mechanism, to be compared to 38 kcal/mol found under OCM conditions. These results may suggest that under OCM conditions the rate-determining step in the reaction sequence to form CO_2 is not the

stepwise dehydrogenation of an hydrogen-containing carbon species but rather the formation of that by the reaction of CH_4 with the catalyst surface. Such a step might be the formation of $CH_3\cdot$ or $-CH_xO$ species.

It is important to note here that at least two steps are rate-determining for the oxidation of carbon species formed by the reaction of C_2H_6 with lattice oxygen. This oxidation is performed under O_2 flow conditions. On the other hand, the oxidation of carbon intermediate species by lattice oxygen, the former produced by CH_4 reaction with lattice oxygen, is controlled by one step only, as discussed in a previous section.

The elementary step 6 of the kinetic model presented, which eventually leads to gas-phase CO_2, is taken as an irreversible step. This implies that adsorption of CO_2 on the catalyst surface or formation of Li_2CO_3 is neglected. We have shown in a previous work (*19*) and discussed before that the present catalyst does not adsorb CO_2 at temperatures higher than 500°C, whereas XPS measurements have shown that lithium segregation to the catalyst surface is small (*19*). Thus, the irreversibility of step 6 of the kinetic model is justified by experimental evidence. Transient experiments with 0.5% CO/6% O_2/He mixture showed that above 700°C CO reacts with the catalyst to form CO_2 whereas the surface coverage of CO is practically zero (*25*). These results may imply that steps 5 and 6 of the kinetic model presented are relatively faster than steps 2–4.

The irreversibility of steps 2–6 and the assumption that a number of these steps have about the same rate constant k, whereas the other steps have a much larger value of k, provided a simple and useful relationship (Eq. (2)) from which kinetic parameters can be extracted. Otherwise, the individual k of each step in the sequence of steps could only be obtained by solving a complex system of differential equations, the latter based on material balances and the kinetics involved in the proposed scheme of steps 1–7. Then, appropriate k values are obtained which best describe the transient responses of Fig. 5. As it was mentioned in a previous section, Eq. (2) of the kinetic model proposed has also been used to explain shifts in the peak maximum of the CH_4 rate observed during isothermal transient hydrogenation of carbonaceous species formed after CO/H_2 reaction (*29*).

The transient CO_2 and C_2H_6 results of Fig. 5, which refer to the oxidation of carbonaceous species formed by C_2H_6/He reaction with the catalyst, contain very important information related to the kinds of adsorbed oxygen species and their reactivity towards the aforementioned carbonaceous species. At first, the fact that the quantity of carbonaceous species removed by O_2 as CO_2 decreases drastically with increasing temperature of reaction in O_2 flow may seem surprising. This behaviour could be attributed to an increase in reactivity of the carbonaceous species formed at 845°C by C_2H_6/He reaction with the catalyst, while the catalyst is cooled to a lower temperature in He flow (transformation to a more active form). If this were true, then one would expect an effect of time in He flow treatment on the reactivity of carbonaceous species. An experiment was conducted which consisted of cooling the reactor from 845 to 707°C during a period of 5 or 40 min, whereas the corresponding experiment shown in Fig. 5a, curve A corresponds to a cooling period of 10 min. The results obtained were identical to those shown in Fig. 5a, curve A. Thus, it is reasonable to exclude the possibility that during the cooling period from 845°C to a lower temperature, before O_2 titration, the reactivity and amount of carbonaceous species had changed. An alternative explanation must, therefore, be sought.

It is suggested that the effect of temperature on the quantity of carbonaceous species removed by O_2 titration (Fig. 5a) can be attributed to two main factors. The first one is the different kind of adsorbed oxygen species, formed by interaction of gas-phase oxygen with oxygen anion vacancies, whose

formation on the catalyst surface depends on temperature. These oxygen species have different reactivity towards the carbonaceous species formed by C_2H_6/He reaction with the catalyst. Oxygen-adsorbed species such as O^-, O_2^-, and O_2^{2-} have been reported to be formed under oxygen treatment conditions of an OCM catalyst (*5*). The second factor is related to the concentration of these adsorbed oxygen species at a given temperature. The higher the concentration, the higher the probability of finding adjacent oxygen sites required for the oxidation of carbonaceous species according to the sequence of steps 2–6 of the kinetic model presented. Thus, the lower the temperature, the higher the concentration of adsorbed oxygen species expected to be formed on the catalyst surface. The increase in the intial oxidation rate with decreasing temperature shown in Fig. 5a, is a strong indication of the validity of the explanation offered above.

The shape of the CO_2 transient at 707°C in Fig. 5a may suggest that more than two kinds of carbon species had been accumulated on the catalyst surface following reaction of C_2H_6/He at 845°C. The presence of these carbon species is probed by O_2 titration at various temperatures (compare curves A and D in Fig. 5a). It should be made clear that the activation energy of 15.3 kcal · mol^{-1} found for the oxidation of these carbon species, calculated based on the observed shift in the peak maximum of CO_2 transient response in Fig. 5a, is associated with one kind of carbon species only, that which almost exclusively reacted with oxygen at 845°C (Fig. 5a, curve D). Thus, reaction of C_2H_6 with lattice oxygen produces more than one kind of carbon species, likely similar to those appeared in the kinetic model proposed.

An important information which can be drawn from the results of Fig. 5a is the exclusion of an Eley–Rideal mechanism for the reaction of gas-phase oxygen with the carbonaceous species to form CO_2. Such a mechanism would have to result in a higher reaction rate and removal of more carbon species with increasing temperature, since the oxygen pressure and the initial coverage of carbon species are kept constant at any temperature. This is exactly the opposite of that observed in Fig. 5a.

Worth of discussion is the appearance of C_2H_6 during the O_2 titration of the carbon species following reaction of C_2H_6/He with the catalyst (Fig. 5b). The assignment of the signal of m/e = 30 to C_2H_6 came after careful examination of the possibility that this signal may also arise from CH_2O. Due to the lack of capability of performing a GC/MS quantitative analysis of the effluent gas from the reactor under dynamic conditions, the following procedure has been applied using only the mass spectrometer detector. The m/e = 26 has been used to identify the presence of C_2H_6, where the CH_2O species does not contribute to the signal of this mass number. The increase of m/e = 26 signal from its background value during the O_2/He titration was indeed observed. If there were no CH_2O in the product stream, and the latter consisted only of C_2H_6, then the ratio of the signals corresponding to m/e = 26 and 30 ought to be the same as that obtained by passing to the mass spectrometer an C_2H_6/He mixture bypass the reactor. This result was indeed observed within 10%. It is also mentioned that (a) no signals due to m/e = 31 and 43 have been observed, indicating that neither CH_3OH, C_2H_5OH, or CH_3CHO are formed during oxygen titration of the carbon species (Fig. 5), and (b) no desorption of C_2H_6 was measured during He purge from 845°C to the O_2 titration temperature. These results may imply that the removal of carbon species by oxygen to form CO_2 releases appropriate sites which are required for the formation of C_2H_6 from its precursor surface species. It is speculated whether an ethoxide species ($OC_2H_5^-$) is the precursor to form C_2H_6 during O_2 titration. This species has been reported to be formed by C_2H_6 reaction with the O^- ions of MgO and lithium-promoted MgO catalysts (*44*, *45*).

Catalytic results of the CH_4/O_2 reaction

over the present Li^+-doped TiO_2 catalyst show that the C_2-hydrocarbons selectivity increases with reaction temperature (*19–21*). This result may be related to the results of Fig. 5, which show that the lower the temperature the larger the amount of carbonaceous species removed by gas-phase oxygen as CO_2. Even though the coverage of carbon species that are in the sequence of steps to form C_2H_6 and CO_x (x = 1,2) is relatively small under OCM conditions over many catalytic systems (*11, 13, 14*), this does not contradict the aforementioned notion.

The shift of the peak maximum of CO_2 response obtained during O_2 titration, following reaction of C_2H_6/He at 845°C for various times on stream (Fig. 4a), could be explained evoking Eq. (I). An increase of t_m could be caused by a decrease in the concentration of oxygen species $[O_x]$. This is very likely to be the case since it was found that the amount of carbon species formed on the surface by C_2H_6/He reaction at 845°C increases with time on stream. Thus, as time on stream increases the concentration of oxygen vacancies blocked by carbonaceous material may increase as well.

CONCLUSIONS

The following conclusions may be drawn from the results of the present investigation:

1. The lattice oxygen of 2 wt% Li_2O-doped TiO_2 catalyst used for the oxidative coupling of methane reaction is found to be a total oxidation site, producing exclusively CO_2, following reaction with CH_4/He. For the case of C_2H_6/He reaction, small amounts of C_2H_4 and CH_4 are formed, whereas the main reaction product is also CO_2. In addition, large amounts of carbonaceous species accumulate on the catalyst surface. Activation energies of 34.0 and 28 kcal · mol^{-1} for CH_4 and C_2H_6 reaction with the lattice oxygen of Li^+-doped TiO_2 catalyst were found, respectively, whereas their transient kinetics were much different.

2. The present CH_4/He transient reaction results suggest that adsorbed oxygen species formed by interaction of gas-phase oxygen with oxygen vacancies of the present catalyst may be responsible for generating $CH_3\cdot$ species that can be dimerized on the surface or in the gas phase to form C_2H_6.

3. Oxygen titration transient results of carbonaceous species formed by C_2H_6/He reaction were interpreted by a kinetic model, based on a sequence of elementary steps. It was found that a stepwise dehydrogenation of these carbonaceous species, $-CH_x$ (x = 0–3) and/or $-CH_xO$ explains well the main features of the O_2 titration transient results.

4. The oxygen titration transient results of carbonaceous species formed by C_2H_6/He reaction at 845°C suggest the presence of more than one kind of adsorbed carbon species with different reactivity. An activation energy of 15.3 kcal · mol^{-1} was calculated for one kind of these carbonaceous species.

ACKNOWLEDGMENT

Financial support by the Commission of the European Community (Contract JOUF-0044-C) is gratefully acknowledged.

REFERENCES

1. Lee, J. S., and Oyama, S. T., *Catal. Rev.-Sci. Eng.* **30,** 249 (1988).
2. Baerns, M., Ross, J., and van der Wiele, Eds., Proceedings of the European Workshop on Catalytic Methane Conversion, Bochum, 1988, Catalysis Today, Vol. 4, 1989. Elsevier Science Publishers, The Netherlands.
3. Bhasin, M. M., *in* "Studies in Surface Science and Catalysis" (D. M. Bibby *et al.*, Eds.), Vol. 36. Elsevier, Amsterdam, 1988.
4. Scurrell, M. S., *Appl. Catal.* **32,** 1 (1987).
5. Dubois, J.-L., and Cameron, C. J., *Appl. Catal.* **67,** 49 (1990).
6. Sokoloskii, V. D., *Catal. Rev.-Sci. Eng.* **32,** 1 (1990).
7. Happel, J., "Isotopic Assessment of Heterogeneous Catalysis." Academic Press, San Diego, 1986.
8. Biloen, P., *J. Mol. Catal.* **21,** 17 (1983).
9. Peil, K. P., Goodwin, J. G., Jr., and Marcelin, G., *J. Phys. Chem.* **93,** 5977 (1989).
10. Ekstrom, A., and Lapszewics, J. A., *J. Am. Chem. Soc.* **110,** 5226 (1988).
11. Peil, K.P., Goodwin, J. G., Jr., and Marcelin, G., *J. Catal.* **131,** 143 (1991).

12. Ekstrom, A., and Lapszewicz, J. A., *J. Phys. Chem.* **93,** 5230 (1989).
13. Kalenik, Z., and Wolf, E. E., *Catal. Today* **13,** 255 (1992).
14. Lacombe, S., Sanchez, J. G., Delichere, P., Mozzanega, H., Tatibouet, J. M., and Mirodatos, C., *Catal. Today* **13,** 273 (1992).
15. Driscoll, D. J., Martir, W., Wang, J.-X., and Lunsford, J. H., *J. Am. Chem. Soc.* **107,** 58 (1985).
16. Tong, Y., Rosymek, M. P., and Lunsford, J. H., *J. Phys. Chem.* **93,** 2896 (1989).
17. Nelson, P. F., Lukey, C. A., and Cant, N. W., *J. Phys. Chem.* **92,** 6176 (1988).
18. Campbell, K. D., and Lunsford, J. H., *J. Phys. Chem.* **92,** 5792 (1988).
19. Efstathiou, A. M., Boudouvas, D., Vamvouka, N., and Verykios, X. E., *J. Catal.*, **140,** 1 (1993).
20. Papageorgiou, D., Vamvouka, D., Boudouvas, D., and Verykios, X. E., *Catal. Today* **13,** 391 (1992).
21. Papageorgiou, D., Efstathiou, A. M., and Verykios, X. E., submitted for publication.
22. Lane, G. S., Miro, E., and Wolf, E. E., *J. Catal.* **119,** 161 (1989).
23. Cant, N. W., Lukey, C. A., and Nelson, P. F., *J. Catal.* **124,** 336 (1990).
24. Lacombe, S., Efstathiou, A. M., Mirodatos, C., and Verykios, X. E., in preparation.
25. Efstathiou, A. M., Papageorgiou, D., and Verykios, X. E., in preparation.
26. Bennett, C. O., *in* "Catalysis under Transient Conditions" (A. T. Bell and L. L. Hegedus, Eds.), Amer. Chem. Soc. Symp. Ser., Vol. 178, p. 1. ACS, Washington, DC, 1982.
27. Stockwell, D. M., and Bennett, C. O., *J. Catal.* **110,** 354 (1988).
28. Efstathiou, A. M., Ph.D. thesis, University of Connecticut, 1989.
29. Bianchi, D., and Gass, J. L., *J. Catal.* **123,** 298 (1990).
30. Korf, S.J., van Ommen, J. G., and Ross, J. R. H., *Prepr.-Am. Chem. Soc. Div.* **35,** 54 (1990).
31. Bytyn, W., and Baerns, M., *Appl. Catal.* **23,** 199 (1986).
32. Nelson, P. F., and Cant, N. W., *J. Phys. Chem.* **94,** 3756 (1990).
33. Renken, A., Müller, M., and Wandrey, C., *in* "Proceedings, 4th International Symposium Chem. React. Eng. Frankfurt, 1976." Amer. Chem. Soc., Washington, D.C. 1976.
34. Bilimoria, M. R., and Bailey, J. E., *ACS Symp. Ser.* **65,** 526 (1978).
35. Wilson, H. D., and Rinker, R. G., *Chem. Eng. Sci.* **37,** 343 (1982).
36. Barshad, Y., Zhou, X., and Gulari, E., *J. Catal.* **94,** 128 (1985).
37. Cutlip, M. B., *AIChE J.* **25,** 502 (1979).
38. Lynch, D. T., *Chem. Eng. Sci.* **39,** 1325 (1984).
39. Barteau, M. A., Ko, E. I., and Madix, R. J., *Surf. Sci.* **104,** 161 (1981).
40. Bonzel, H. P., and Ku, R., *Surf. Sci.* **33,** 91 (1972).
41. Sarkany, J., Bartok, M., and Gonzalez, R. D., *J. Catal.* **81,** 347 (1983).
42. McCabe, R. W., and Schmidt, L. D., *Surf. Sci.* **60,** 85 (1976).
43. Efstathiou, A. M., and Bennett, C. O., *J. Catal.* **120,** 118 (1989).
44. Morales, E., and Lunsford, J. H., *J. Catal.* **118,** 255 (1989).
45. Alka, K.-I., and Lunsford, J. H., *J. Phys. Chem.* **81**(14), 1393 (1977).